

# Hybrid hydrogen-battery systems for renewable off-grid telecom power

D Scamman, M Newborough\*, H Bustamante  
ITM Power

\*Corresponding author: [mn@itm-power.com](mailto:mn@itm-power.com)

## Abstract

Off-grid hybrid systems, based on the integration of hydrogen technologies (electrolysers, hydrogen stores and fuel cells) with battery and wind/solar power technologies, are proposed for satisfying the continuous power demands of telecom remote base stations. A model was developed to investigate the preferred role for electrolytic hydrogen within a hybrid system; the analysis focused on powering a 1kW telecom load in three locations of distinct wind and solar resource availability. When compared with otherwise equivalent off-grid renewable energy systems employing only battery energy storage, the results show that the integration of a 1kW fuel cell and a 1.6kW electrolyser at each location is sufficient, in combination with a hydrogen storage capacity of between 13 and 31kg, to reduce the required battery capacity by 54-77%, to increase the minimum state-of-charge from 37-55% to >81.5% year-round despite considerable seasonal variation in supply, and to reduce the amount of wasted renewable power by 55-79%. For the growing telecom sector, the proposed hybrid system provides a 'green' solution, which is preferable to shipping hydrogen or diesel to remote base stations.

## Keywords

Telecom;  
Off-grid;  
Electrolysis;  
Hybrid hydrogen-battery energy storage;  
Renewable storage;

## Highlights

- Remote telecom base stations require continuous power from variable renewables
- Renewable energy systems require energy storage to manage large supply fluctuations
- Batteries exhibit short lifetimes in renewable energy systems
- Integrating hydrogen energy facilitates close regulation of battery state-of-charge
- Hybrid hydrogen-battery systems provide a more reliable solution for off-grid power

37 **1. Introduction**

38 The world faces a revolution in energy systems as it seeks to satisfy a growing global energy demand from  
39 an increasing population while dramatically reducing greenhouse gas emissions. In some regions and  
40 some applications, off-grid energy systems powered by renewables could contribute to the 2050 goal of  
41 cutting carbon emissions by  $\geq 80\%$  relative to 1990. Such systems gradually become more affordable as  
42 manufacturing production rates increase. For example the IEA indicates that solar photovoltaic power  
43 sources could overtake coal power sources by 2050 by making a 27% contribution to the total supply,  
44 which when considered in conjunction with hydro, wind and biomass the total renewables contribution  
45 could amount to 79% [1]. In Asia, Africa and the Middle East, plentiful resources and a lack of existing  
46 infrastructure could allow many developing countries to apply off-grid systems for decentralised power.  
47 For example, sub-Saharan Africa's population is expected to double to 1.75 billion by 2040 with energy  
48 demand increasing by 80%, but leaving 530m people without power, primarily in rural communities.  
49 Renewables are expected to provide two-thirds of the capacity in mini-grid and off-grid systems in these  
50 rural areas where low population density makes grid connection uneconomic [2].

51  
52 One early market where global demand is showing considerable growth is telecommunications. The  
53 requirement for more widespread use of remote base stations is becoming increasingly important with  
54 3G and 4G networks in emerging markets and the added advantage of not requiring the installation of a  
55 telephone cable network. China has the world's largest mobile telecommunications network with over 1  
56 million telecommunications base stations, a number which is growing at ten to twenty thousand *p.a.* [3].  
57 Telecom towers, by their nature, are often positioned in remote locations where reliable grid electricity  
58 is not present and network operators have no option but to pursue alternative power sources. Diesel-  
59 fuelled generators suffer from low efficiency, the high costs of fuel replacement and delivery, the emission  
60 of carbon dioxide and other pollutants, and the risk of fuel theft and degradation. Hence there is a  
61 growing interest in the use of renewable power sources by telecom stations in order to replace diesel [4]  
62 [5]. One recent study estimated that by 2020 there could be 400,000 off-grid telecom base stations  
63 operating on renewable power, particularly in remote parts of the developing world, with an associated  
64 market size of \$10.5 billion *p.a.*, [6].

65  
66 Telecom applications require an extremely reliable 24-hour supply of power, resulting in the need for  
67 energy storage for providing backup power during grid outages or primary power during lulls in wind or  
68 solar photovoltaic (PV) generation. Historically this has been performed primarily by batteries for backup  
69 power (*i.e.* to cover a defined period of failure in the primary power system) [7] [8] [9] [10], with \$4.7 to  
70 \$7.9 billion of battery sales per year recorded in China for the telecom industry alone [3]. Lead acid  
71 batteries are the main technology used in off-grid systems due to their maturity and low cost. However  
72 'battery-only' solutions have uncertain life expectancies, especially for off-grid applications at sites with  
73 large seasonal variations in renewable power production. In such systems batteries encounter long  
74 periods at a low state-of-charge (SOC), numerous partial cycles at low SOC and other periods at full charge  
75 so preventing the absorption of available renewable electricity. These factors negatively affect battery  
76 lifetime [11] [12] [13] [14] and distinguish the telecom application from automotive, portable or  
77 uninterrupted power supply applications where deep discharges are experienced but then batteries tend  
78 to be quickly recharged and remain near full charge for much of their working lives. Self-discharge  
79 mechanisms over time serve to reduce a battery to a partially-charged state, reducing its life expectancy  
80 and making it unsuitable for seasonal storage. In a well-designed system with appropriate maintenance  
81 batteries can last up to 15 years, but they have been found to fail after only a few years in systems served  
82 by solar/wind power. This makes battery lifetime quite short compared to other system components,  
83 leading to system unreliability and frequent replacements, making batteries a weak link in remote  
84 telecom systems [11] [12] [13] [15]. In general batteries are best operated at high SOC to optimise

85 lifetime, as discharging at low SOC degrades batteries more than discharging at high SOC [16]. Some  
86 manufacturers have responded by designing deep-cycle batteries specifically for remote power  
87 applications, but the potential for extending battery life this way is limited. Whichever battery chemistry  
88 is used, there is considerable potential for a solution which can extend battery life by maintaining the SOC  
89 within a limited range year-round (e.g. 80-100%).

90  
91 Interest in the use of hydrogen, as an alternative to batteries and diesel-fuelled generators, is growing for  
92 telecom power [4] [5] [9] [10]. Existing commercial solutions ('hydrogen-only' systems) require bottled  
93 hydrogen to be delivered to site [17] [18] [19]. This hydrogen tends to be characterised by a high carbon  
94 footprint because it is usually produced centrally via steam methane reformation, then compressed and  
95 transported by diesel truck. Alternatively hydrogen-only systems may be powered by on-site renewables,  
96 but these are inhibited by the poor round trip efficiency of an electrolyser/fuel-cell combination, which  
97 forces the specification of high capacities for the power source, electrolyser and hydrogen store.  
98 Therefore hybrid off-grid systems, and the complex sizing, storage and control challenges they present,  
99 are receiving considerable research attention [20] [21] [22].

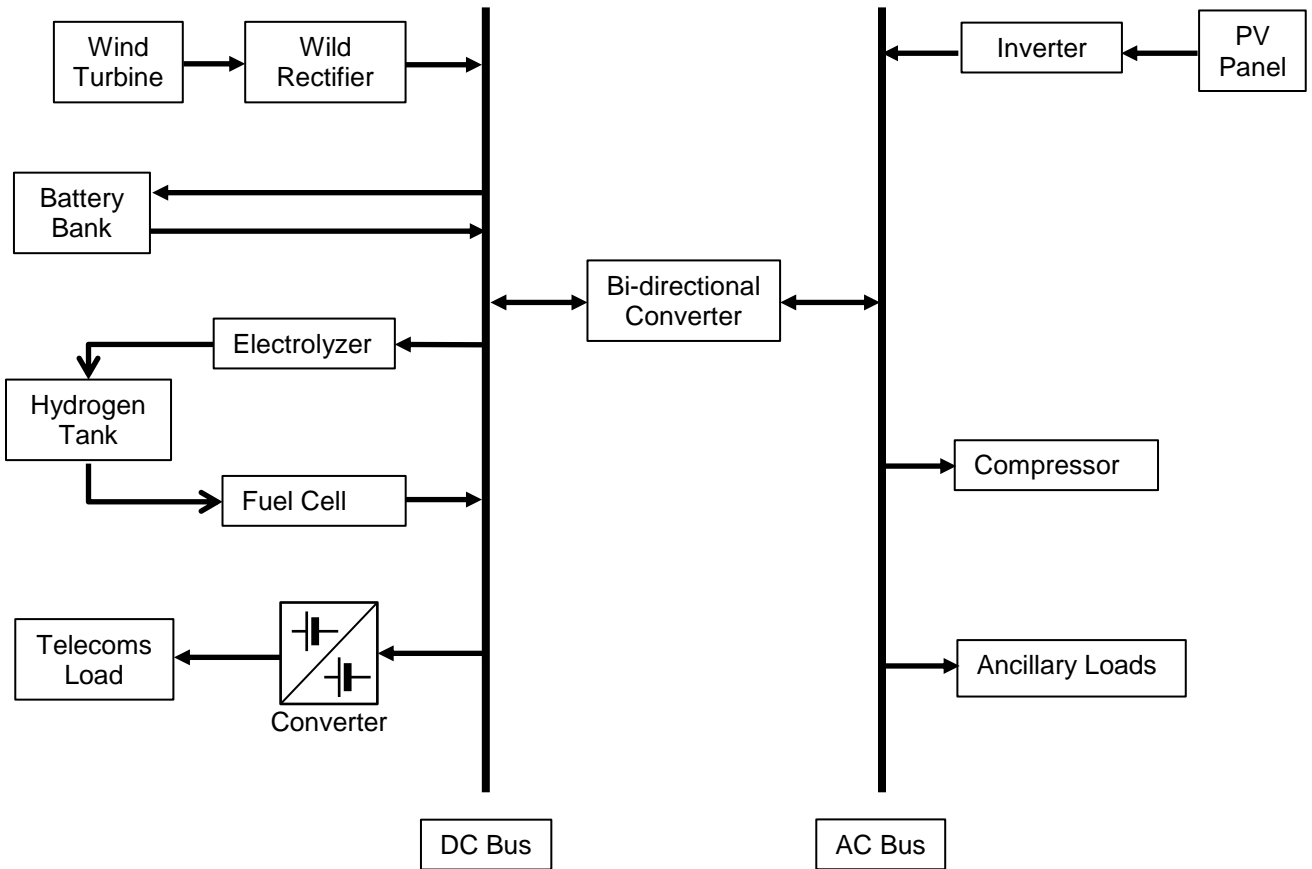
100  
101 Previous investigators have noted that, in systems incorporating hydrogen storage, hydrogen is ideal for  
102 seasonal bulk energy storage while batteries are best suited for short-term storage [23]. PV-powered  
103 systems incorporating fuel cells and batteries have been found to achieve lower costs and lower PV  
104 requirements than battery-only and hydrogen-only systems based on delivered hydrogen [21]. Telecom  
105 applications usually need 3-5 days of backup to navigate periods of cloudy weather, and fuel cells are able  
106 to offer longer runtimes than batteries (because hydrogen storage tanks are scalable) as well as  
107 environmental benefits due to a reduced reliance on lead-acid systems [3]. Hybrid systems have been  
108 found to be cheaper than battery-only systems due to lower O&M costs, and with greater efficiency and  
109 reliability than hydrogen-only systems [24]. Previous studies of hybrid hydrogen-battery storage systems  
110 have shown that heavy battery use can lead to more efficient systems with reduced PV/wind  
111 requirements, but with deep discharges and/or long periods at low SOC which adversely affect battery  
112 life [17] [19] [25]. Others have shown that batteries can be protected through reduced usage by placing  
113 a heavy reliance on hydrogen, but with adverse impacts on system efficiency and renewable power  
114 capacity [20] [26] [27]. Here we show that a compromise can be reached, with batteries improving system  
115 efficiency and reducing PV/wind capacity requirements through regular daily cycling, while the hydrogen  
116 component serves to maintain battery SOC within narrow limits and so extend battery life.

117  
118 We propose a hybrid system for off-grid telecom power comprising on-site hydrogen generation by  
119 electrolysis, gaseous hydrogen storage and power generation by a PEM fuel cell. The hydrogen  
120 technologies are integrated with batteries and a renewable power source(s) to form a 'hydrogen-battery'  
121 system. This hybrid configuration, which may be compared with a conventional 'battery-only' system,  
122 provides an off-grid solution based entirely on renewable energy. Wind and/or solar energy can be either  
123 stored in the battery, or used by the electrolyser to produce hydrogen for storage and later use by the  
124 fuel cell. The fuel cell and battery work together to ensure year-round uninterrupted power for the  
125 telecom application, while the electrolyser and battery function to capture the electricity generated by  
126 the on-site renewable power source(s). The envisaged operating logic is for the hydrogen technologies to  
127 support the battery technology, with the hydrogen store providing a seasonal buffer. The foremost design  
128 challenge is to identify the capacities and operating regimes of the power source(s), battery, electrolyser  
129 and fuel cell for site locations with characteristically different solar and wind regimes. Although an  
130 economic analysis was beyond the scope of this investigation, it was assumed that reducing the capacities  
131 of the hydrogen technologies (electrolyser, hydrogen storage facility, hydrogen compressor and fuel cell)  
132 should make the capital cost of the proposed system more acceptable. Furthermore, the proposed

133 approach can provide a greener solution than existing off-grid telecom systems employing fuel cells,  
 134 because these require compressed hydrogen to be shipped in at regular intervals by diesel truck.  
 135 Accordingly, new markets can be achieved for small PEM electrolyzers in the telecom sector.  
 136

137 **2. Hybrid System Design**

138 The basic system architecture enables the deployment of both PV and wind power sources at the telecom  
 139 site (Figure 1). The design consists of an AC bus and a DC bus joined by a bi-directional converter. Power  
 140 from the wind turbine is fed to the DC bus through a wild rectifier needed to smooth unsteady turbine  
 141 output. The PV panel voltage varies as it tracks the maximum power point, requiring conversion to reach  
 142 the bus voltage, and power is fed through an inverter to the AC bus. Separate AC and DC buses enable  
 143 maximum power point tracking for both the wind turbine and the PV array. The DC telecom load is  
 144 connected to the DC bus to reduce conversion losses, and it receives power from the battery, the fuel cell,  
 145 the wind turbine and/or the PV panel. The renewable power output is absorbed by the load, battery and  
 146 electrolyser with excess renewables stored firstly in the battery to raise SOC, and secondly as hydrogen  
 147 once the battery is full. Small ancillary AC loads (data logging, ventilation, communication etc.) are  
 148 connected to the AC bus. This system configuration was analysed for sites where the deployment of one  
 149 or both types of renewable power source was feasible (Section 4).  
 150  
 151



170 Figure 1: Hybrid system layout

171  
 172 **2.1 Telecom Load and Fuel Cell Capacity**

173 The total power requirement was assumed to be a continuous total load of 1kW, including the ancillary  
174 AC loads and conversion losses from the DC bus. This is a typical size for remote telecom systems [5]. The  
175 constancy of the load enabled a simple sizing decision to be made for the fuel cell, which was fixed at  
176 1.0kW, so that it could meet the total power requirement in the event of a failure of the battery or  
177 wind/solar power sources (so improving system reliability). It was assumed that the fuel cell would only  
178 be operated at full load; its conversion efficiency (including DC-DC conversion) was taken as 50% (LHV) at  
179 rated power, a value readily achievable with commercial systems [28]. One advantage of a telecom  
180 system compared with other off-grid systems is that it doesn't require the fuel cell to be sized to meet a  
181 peak load that occurs only briefly and intermittently.

182

## 183 **2.2 PV Panels**

184 Given the low capacity factor of solar energy and the energy conversion losses within the hybrid system,  
185 the solar photovoltaic power source (PV) needs to be of much greater capacity than the load. The required  
186 PV capacities for various site locations were estimated using the system model. The method used for  
187 estimating the electricity yield has been reported previously [29]. Irradiance levels for the locations  
188 analysed were estimated using the HOMER modelling package [30]. This synthesises hourly irradiance  
189 data onto a horizontal plate from the 22-year (1983-2005) NASA Surface meteorological and Solar Energy  
190 (SSE) dataset [31]. Irradiance levels were adjusted to account for shading, ground reflectance, ageing and  
191 cable loss effects. The PV panels were implemented at the latitude tilt angle and orientated to face due  
192 south to improve yield. The PV power output was assumed to be net of inverter losses.

193

## 194 **2.3 Wind Turbine**

195 Wind turbine power output was also estimated using HOMER. The turbine power curve was based on a  
196 Proven 6 kW turbine (with a 15 m hub height and a 90% efficient rectifier [32]), and it was scaled linearly  
197 with capacity where the model recommended small deviations from the 6 kW value. Monthly wind-  
198 speeds were linearly interpolated from the University of East Anglia's Climate Research Unit CL v2.0  
199 dataset, derived from 1961-1990 monthly means and reported at 10-minute resolution and 10m above  
200 ground level [33]. Hourly wind-speed values were synthesized from this dataset in HOMER using typical  
201 values of 0.01m surface roughness length, 0.85 autocorrelation factor, 0.25 diurnal pattern strength,  
202 14:00 time of peak wind speed and a Weibull factor that scales linearly with average wind speed. One  
203 such turbine is normally sufficient for telecom systems.

204

## 205 **2.4 Electrolyser and Hydrogen Storage**

206 The electrolyser model was based on a novel proton-exchange membrane (PEM) electrolyser designed  
207 for generating hydrogen from a renewable power source off-grid [29]. The electrolyser self-pressurises to  
208 15 bar and incorporates a passive operating mechanism for achieving a very low balance-of-plant power  
209 consumption. It is more efficient at part-load than full load (Figure 2), enabling hydrogen to be produced  
210 with high efficiency at low input power levels. The electrolyser capacity was fixed at 1.6kW at which it  
211 achieved a stack efficiency of 75% (HHV); the minimum operating point was taken as 10% of full capacity  
212 (i.e. 0.16kW), at which it achieved a stack efficiency of 93% (HHV), with power levels below this sent to  
213 the battery.

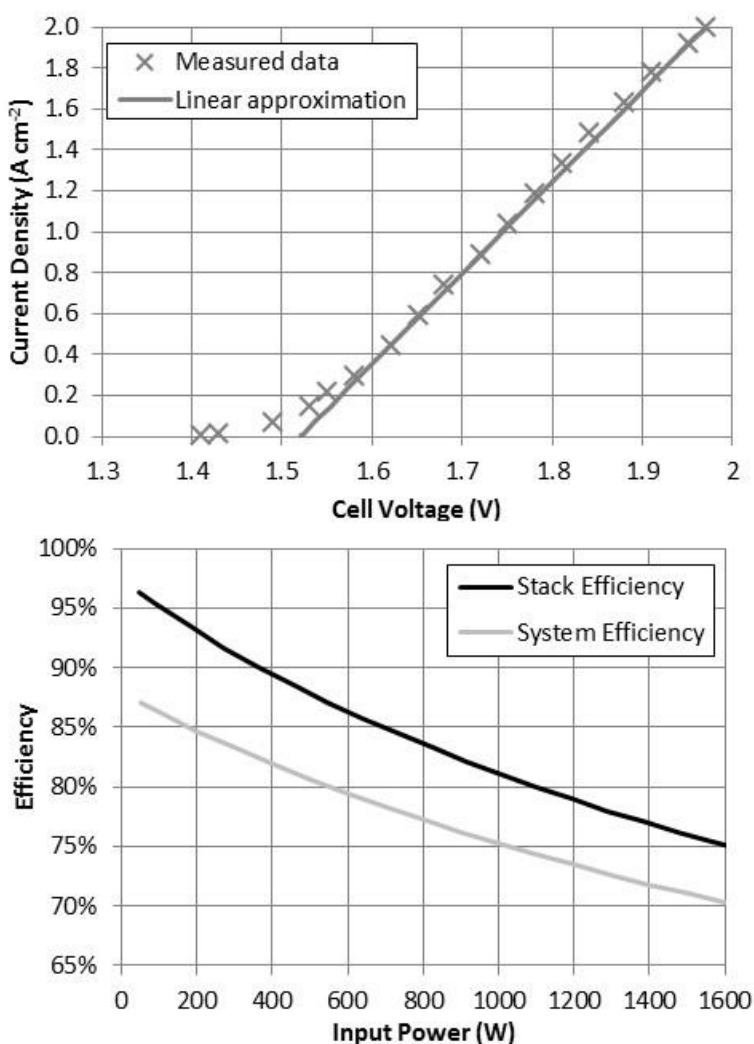
214

215 It was assumed that the product hydrogen from the electrolyser would be accumulated in a 15 bar buffer  
216 store then compressed for storage in conventional 200 bar steel cylinders. This requirement for gas  
217 compression is driven by the space available at the telecom site. Given the hydrogen generation pressure  
218 of 15 bar, it was considered that any capacity requirement of >10kg H<sub>2</sub> would make the use of a gas  
219 compressor essential, in order to limit the system footprint. Additionally a minimum storage level of 1 kg  
220 was specified, which allows approximately 17 hours of fuel cell operation in the event of an emergency.

221 A value for the compression work  $w_c$  from 15 bar of 4.35 kWh/kg was used, calculated from the relation  
 222 below derived from the ideal gas equation for isothermal compression at 293 K with an ideal gas constant  
 223 R of 8.31 kJ kmol<sup>-1</sup> K<sup>-1</sup>, relative molecular mass of hydrogen RMM<sub>H<sub>2</sub></sub> of 2.016 kg kmol<sup>-1</sup> and a compression  
 224 efficiency  $\eta_c$  of 20%. Inaccuracies in the compression work value resulting from deviations from the ideal  
 225 gas equation are thought to be small compared with the uncertainties in the value of compression  
 226 efficiency, which can vary considerably with the compression technology used. The compressor work is  
 227 subtracted from the electricity otherwise employed for electrolysis as shown in Appendix A. This results  
 228 in an electrolyser system efficiency of about 70% (HHV) at a power input of 1.6 kW, which increases at  
 229 part-load (Figure 2).

$$w_c = \frac{RT}{3600\eta_c RMM_{H_2}} \ln \frac{p_2}{p_1} \quad (1)$$

230



231

232 Figure 2: Electrolyser performance

233 **2.5 Batteries**

234 Because of their higher round trip efficiency, the batteries were sized to meet the majority of the electrical  
235 work done. The battery model was based on Rolls 4KS25P deep-discharge batteries which are available in  
236 capacities of up to 7.6 kWh at low discharge rates [34]. The round-trip efficiency was taken as 80%, with  
237 a 2% per month self-discharge rate typical for lead-acid batteries. The battery SOC value was computed  
238 by dividing the energy stored (and available for discharge when required) by the maximum discharge  
239 capacity of the battery. The model assumed simple constant current charging of the battery.

240

### 241 **3. Model**

242 A model evaluated at hourly intervals was developed to explore the effect of different size components  
243 on the performance of the hybrid system. The design objectives were as follows.

244

- 245 • Manage the temporal variations in the renewable power supply and in the charge levels of the battery  
246 and hydrogen stores, to ensure the telecom load can be met year-round, and so define a design  
247 solution for the hybrid system.
- 248 • Maintain the battery close to a high SOC 'ceiling level' and avoid leaving it for long periods at a low  
249 SOC 'floor level', in order to prolong battery life.
- 250 • Minimise the required PV/wind capacity, hydrogen storage capacity and battery capacity to reduce  
251 system costs and footprint.
- 252 • Enable renewable power generation in excess of the electrolyser capacity to charge the battery. This  
253 allows a smaller electrolyser capacity to be used.
- 254 • Minimise curtailment of the renewable power source without oversizing other system components,  
255 which are then under-utilised for the rest of the year.
- 256 • Maintain a hydrogen store charge level sufficient to (i) guarantee year-round operation, (ii) provide  
257 emergency telecom availability in the event of a systems failure and (iii) allow maintenance without  
258 necessarily interrupting operation of the telecom system.

259

260 To achieve this, the electrolyser absorbs up to 1.6kW of renewables supply in excess of the telecom load,  
261 provided that there is sufficient room in the hydrogen store to accommodate the gas produced and the  
262 battery is at its SOC ceiling. This ceiling was chosen to be typically 95-98% of full charge; high enough to  
263 prioritise maintaining the battery at the highest SOC's possible, whilst leaving some headroom for the  
264 battery to absorb subsequent additional renewables input if available (on the next sunny day, for  
265 example). The battery absorbs any renewables supply in excess of the combined electrolyser and telecom  
266 load. If the battery is fully charged and the electrolyser is operating at full capacity, any additional  
267 renewable supply is curtailed; the model aims to minimise the amount of curtailed renewables, though  
268 some wastage is inevitable.

269

270 The battery discharges the amount required to meet the telecom load if there is insufficient renewables  
271 supply. If the battery SOC drops below a chosen SOC floor value, the fuel cell is subsequently switched on  
272 to prevent deep discharging of the battery. Any incoming renewable power then powers the telecoms  
273 load directly, with the fuel cell picking up any shortfall. As the fuel cell output is fixed at 1 kW, any excess  
274 fuel cell generation above that used to power the telecoms load then recharges the battery; if incoming  
275 renewables in fact exceeds 1 kW, the model records this as 1 kW of renewables powering the telecom  
276 load and 1kW of fuel cell output (and any additional renewables) recharging the battery, in order to  
277 elevate the SOC as quickly as possible. Incorporating a weather forecasting capability could allow an  
278 operator to decide to operate the fuel cell on the basis of upcoming renewables production, but this was  
279 beyond the scope of the current investigation. Once the battery SOC exceeds the SOC floor value, the  
280 fuel cell is switched off to conserve hydrogen. The model did not impose a minimum runtime on the fuel

281 cell, so sometimes it switched off after only one hour. The fuel cell never operated if the electrolyser was  
282 running or the battery was discharging. The SOC floor value was chosen to be typically 80%; high enough  
283 to protect the battery from deep discharge, but low enough to prevent emptying the hydrogen store  
284 prematurely.

285  
286 There is considerable scope to adjust the SOC floor value (to start the fuel cell) and the ceiling value (to  
287 start the electrolyser). Raising these values increases the battery SOC level but can empty the hydrogen  
288 store prematurely, requiring an increased renewable power capacity to make up the short-fall. The model  
289 permitted the use of separate winter and summer floor/ceiling values to respect the variation in  
290 renewable supply, but it was found that similar summer and winter values were able to maintain high SOC  
291 levels year-round. Ultimately a system could incorporate updated weather forecasts to predict when  
292 renewables availability will be low and fuel cell operation is required to prevent SOC dropping too low, or  
293 when the electrolyser should be operated to create battery headroom to fully absorb renewables on an  
294 upcoming windy or sunny day.

295  
296 The model demonstrated that component sizing was determined by a number of competing factors. For  
297 example, PV and wind turbine capacities were kept low to reduce costs, but high enough to ensure that  
298 final tank and battery levels matched their initial values. Battery SOC was kept high year-round, and the  
299 amount of shed renewables was kept low. The hydrogen storage capacity was kept low to reduce costs,  
300 but it had to be large enough to capture as much renewable supply as possible during plentiful periods to  
301 help maintain battery SOC during leaner times of the year. The number of batteries was also kept low to  
302 reduce costs, but high enough to avoid deep discharges with the aid of the hydrogen storage system. The  
303 component sizes reported here satisfy these design constraints; a cost model would allow these to be  
304 optimized further.

305  
306 To demonstrate the benefits of the hybrid hydrogen-battery system, it was compared with an otherwise  
307 equivalent battery-only system. Adding hydrogen storage will improve the reliability of any existing  
308 system simply by virtue of adding more energy storage capacity, so for a valid comparison the number of  
309 batteries in the battery-only system was increased by an amount equivalent to the energy stored as  
310 hydrogen in the hybrid system. For example, 5 kg of hydrogen generates 83 kWh<sub>e</sub> through a 50% efficient  
311 fuel cell, which is equivalent to about eleven 7.6 kWh<sub>e</sub> batteries. The PV/wind capacity was also kept the  
312 same for the battery-only system to allow like-for-like comparisons, although it is acknowledged that a  
313 system designer could choose to install slightly smaller power sources to reduce capital expenditure and  
314 incur worse minimum and average SOC values than reported here.

315

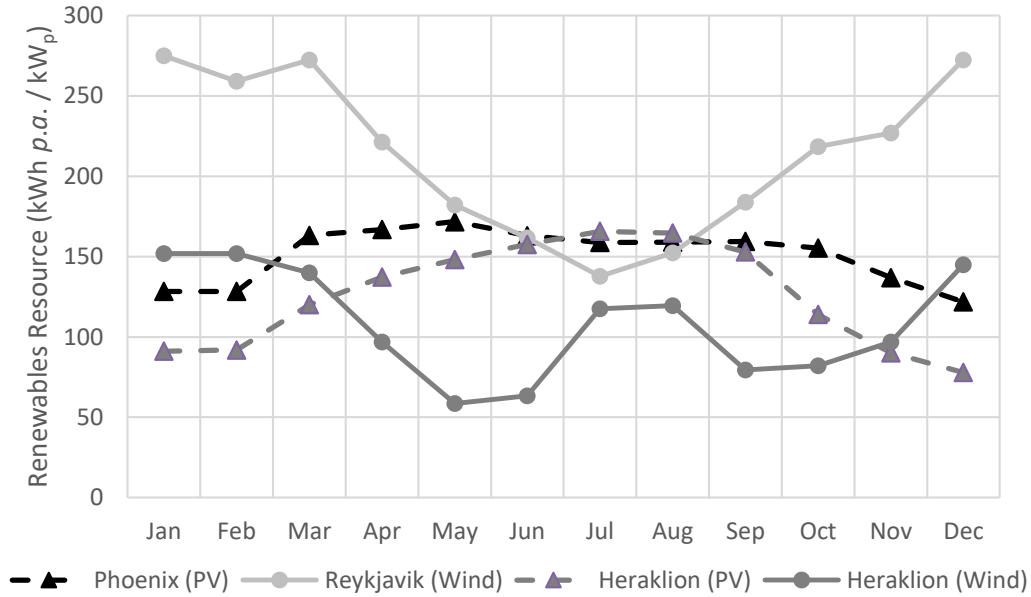
### 316 **3.1 Location Selection**

317 Three sites for analysis were chosen because of their significant but distinct renewables resource profiles  
318 (Phoenix, Arizona; Heraklion, Crete; and Reykjavik, Iceland). Phoenix was selected for its high solar  
319 resource, while Reykjavik was chosen for its high wind-speeds. Both have significant seasonal swings in  
320 their renewable supply, with PV output peaking in Phoenix in the summer and wind generation peaking  
321 in Reykjavik in the winter (Figure 3). Heraklion, which is of similar latitude to Phoenix, was selected  
322 because it has both a significant solar and wind resource. Heraklion has a peak in solar availability in the  
323 summer and a peak in wind supply in the winter, with additional significant summer breezes in July and  
324 August (Figure 3).

325  
326 The total PV resource for Phoenix was estimated at 1,813 kWh *p.a.* / kW<sub>p</sub> (Table 1), which is high for PV  
327 systems. The total wind resource for Reykjavik was 2,563 kWh *p.a.* / kW<sub>p</sub>, which is high for small, onshore



328 installations. The PV resource for Heraklion was 1,511 kWh p.a. / kW<sub>p</sub>, while the wind resource was 1,303  
 329 kWh p.a. / kW<sub>p</sub> (which is much lower than for Reykjavik but still significant).  
 330



331

332 Figure 3: Seasonal variation in renewables resource

333 **4. Results and Discussion**

334 The required component sizes found for the three sites are shown in Table 1. Results are shown firstly for  
 335 the baseline battery-only system, and secondly for a hybrid hydrogen-battery system with the same  
 336 capacity of renewable generation but where some of the battery storage has been replaced with hydrogen  
 337 storage. The PV-only site (Phoenix) required 6.25 kW of PV and 65 batteries for its battery-only system,  
 338 and had an average battery SOC over the course of a year of 90.0% with a minimum SOC of 54.7%,  
 339 spending over 4 consecutive months without a full charge (Figure 4). The battery store experienced a  
 340 total of 1,948 hours p.a. (22.2% of the year) below 80% SOC. Replacing 35 of the batteries with an  
 341 equivalent 17 kg of hydrogen storage raised the annual average battery SOC to 95.2% with a much higher  
 342 minimum SOC of 85.9%. The hydrogen store reached its minimum 1 kg reserve level in February before  
 343 filling up over the summer, reaching maximum capacity at the end of October before emptying again over  
 344 the winter (Figure 4). The battery SOC was a little lower in winter when renewable power generation was  
 345 scarcer, but remained above 85% SOC throughout the year with regular full charges.

346

347

	Phoenix		Reykjavik		Heraklion	
	Battery-only	H <sub>2</sub> -Battery	Battery-only	H <sub>2</sub> -Battery	Battery-only	H <sub>2</sub> -Battery
PV resource (kWh <i>p.a.</i> / kW <sub>p</sub> )	1,813	1,813	-	-	1,511	1,511
Wind resource (kWh <i>p.a.</i> / kW <sub>p</sub> )	-	-	2,563	2,563	1,303	1,303
PV capacity (kW)	6.25	6.25	-	-	3	3
Wind capacity (kW)	-	-	4.5	4.5	4.75	4.75
Hydrogen storage capacity (kg)	-	17	-	31	-	13
Number of batteries*	65	30	86	20	63	25
Battery capacity (kWh)	497	228	656	152	480	190
Average battery SOC (%)	90.0	95.2	81.0	93.6	87.9	92.0
Minimum battery SOC (%)	54.7	85.9	36.7	85.5	54.5	81.5
Hours <i>p.a.</i> at < 80% SOC	1,948	0	3,121	0	2,820	0
Electrolyser start-ups per year	-	226	-	298	-	208
Average electrolyser runtime (h)	-	3.6	-	6.4	-	5.1
Fuel cell start-ups per year	-	54	-	231	-	120
Average fuel cell runtime (h)	-	6.4	-	3.2	-	3.4

348 \* Rolls 4KS25P deep-discharge batteries of 7.6 kWh capacity [34]

349 Table 1: Component sizes for the hybrid and battery-only systems

350 The monthly variations in energy production (both PV generation and discharging of the battery and fuel  
351 cell), and consumption (by the telecoms load, battery and electrolyser) are shown in Figure 5, with annual  
352 totals shown in Table 2. Electrolyser operation occurred mainly in the summer months to fill the hydrogen  
353 store with excess PV energy, with 1,149 kWh sent annually to the electrolyser versus 5,865 kWh sent to  
354 the battery (*i.e.* 16.4% of the total sent to storage). A low average runtime of 3.6 hours per start-up  
355 indicates that surplus PV generation occurs only for short periods. Fuel cell operation occurred mainly in  
356 winter to cover the valley in PV production, with the majority of the generated electricity (292 kWh) used  
357 to power the telecoms load directly and the remainder (53 kWh) to recharge the depleted battery. Using  
358 the fuel cell to recharge the battery this way reduces system efficiency slightly, but should increase battery  
359 longevity. A long average fuel cell runtime of 6.4 hrs per start-up indicates that the fuel cell often had to  
360 run overnight due to the lack of PV generation. Accordingly only 43% of the telecom power requirement  
361 could be met directly by the power source (Figure 6) with the remainder coming from the battery or the  
362 fuel cell. Likewise only 33% of PV generation could be used by the telecoms load directly, with the majority  
363 of the remainder stored for use later (Figure 7). This demonstrates the high usage of batteries for daily  
364 cycling in PV systems, and hence the need for regular cycling to occur at elevated SOC if a long battery life  
365 is to be achieved. The battery round-trip efficiency was slightly below 80% due to self-discharge.  
366 Curtailment of PV production was limited to 531 kWh (4.7% of total annual production) in the hybrid  
367 system, and it occurred primarily in the summer months. This is less than half the 1,191 kWh of  
368 curtailment required by the battery-only system (10.5% of its total annual production) which spends most  
369 of the summer at 100% SOC, unable to accept any excess PV.

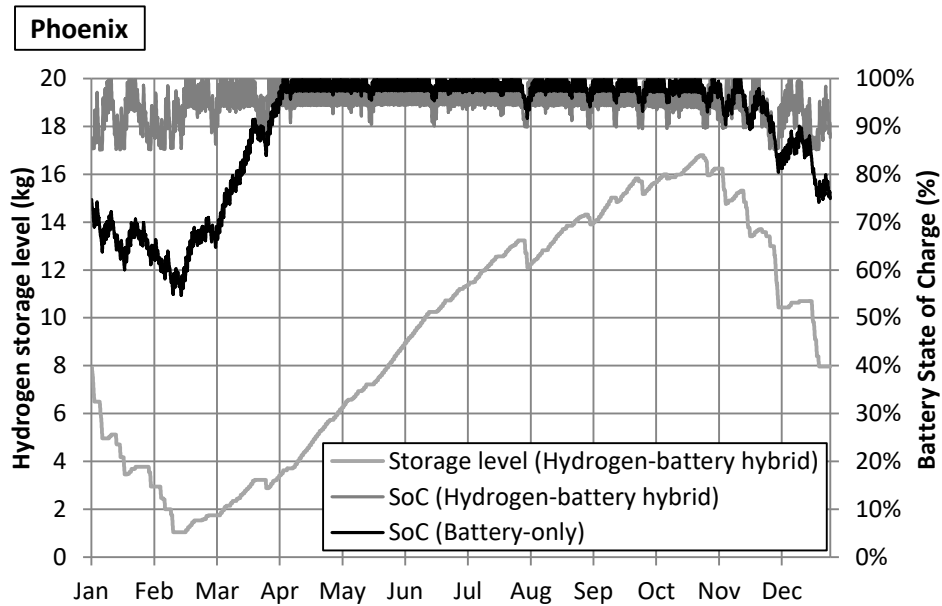
370

371

			Battery-only Storage System				Hydrogen-Battery Hybrid Storage System				
			Consumption (kWh p.a.)			Total Production (kWh p.a.)	Consumption (kWh p.a.)				Total Production (kWh p.a.)
			Telecoms Load	Battery In	Shed Renewables		Telecoms Load	Battery In	Electrolyser	Shed Renewables	
Phoenix	Production (kWh p.a.)	PV Generation	3,785	6,354	1,191	11,330	3,785	5,865	1,149	531	11,330
		Battery Out	4,975	-	-	4,975	4,683	-	-	-	4,683
		Fuel Cell	-	-	-	-	292	53	-	-	345
	Total Consumption (kWh p.a.)	8,760	6,354	1,191	16,305	8,760	5,918	1,149	531	16,358	
Reykjavik	Production (kWh p.a.)	Wind Generation	6,026	3,579	1,928	11,533	6,026	2,588	2,439	480	11,533
		Battery Out	2,734	-	-	2,734	2,208	-	-	-	2,208
		Fuel Cell	-	-	-	-	526	215	-	-	741
	Total Consumption (kWh p.a.)	8,760	3,579	1,928	14,267	8,760	2,803	2,439	480	14,482	
Heraklion	Production (kWh p.a.)	PV Generation	2,153	2,044	337	4,534	2,153	1,848	472	61	4,534
		Wind Generation	3,225	2,287	676	6,188	3,225	1,955	857	151	6,188
		Battery Out	3,382	-	-	3,382	3,093	-	-	-	3,093
		Fuel Cell	-	-	-	-	289	116	-	-	405
	Total Consumption (kWh p.a.)	8,760	4,332	1,013	14,104	8,760	3,919	1,329	212	14,220	

372 Table 2: Energy flows for battery-only and hybrid systems

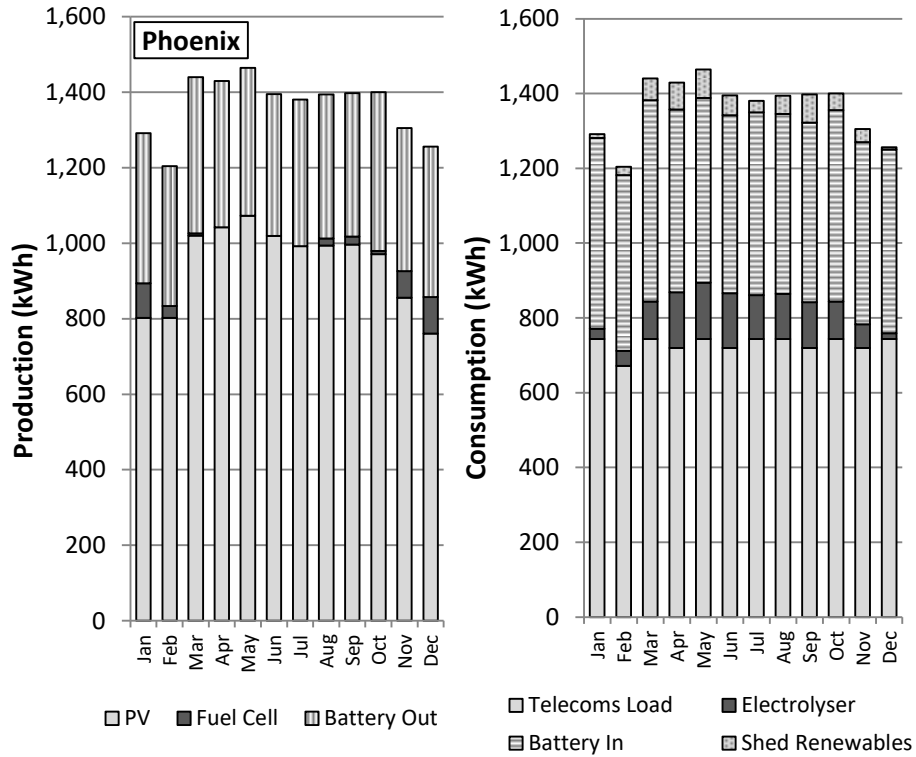
373



374

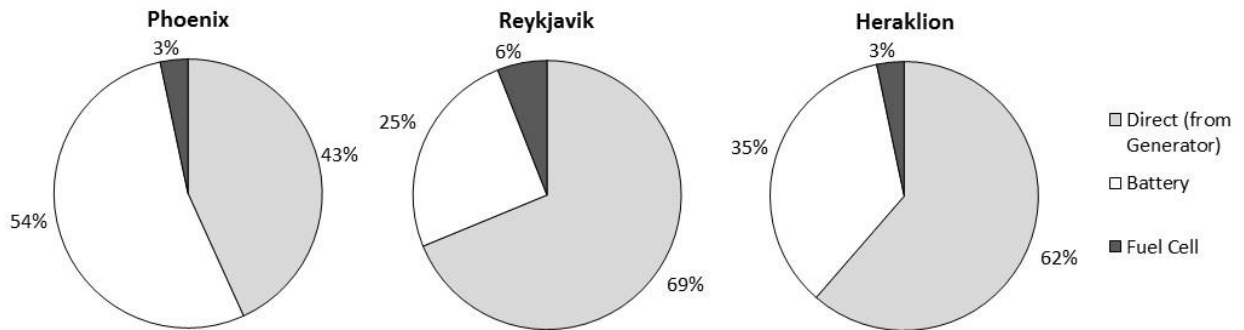
375 Figure 4: Hydrogen storage level and battery SOC variations (Phoenix)

376



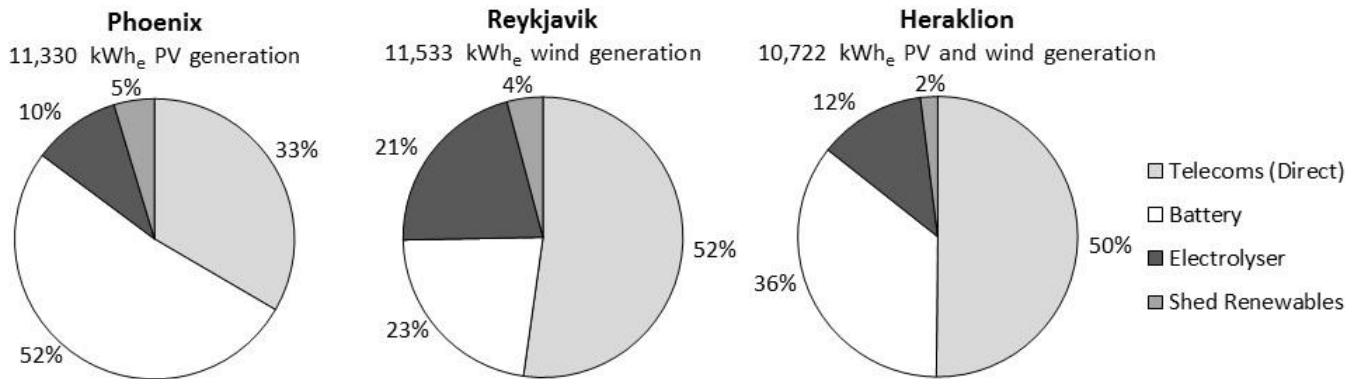
377

378 Figure 5: Monthly variations in electricity production and consumption (Phoenix)



379

380 Figure 6: Source of telecoms power in hybrid hydrogen-battery system (8,760 kWh p.a. total)



381

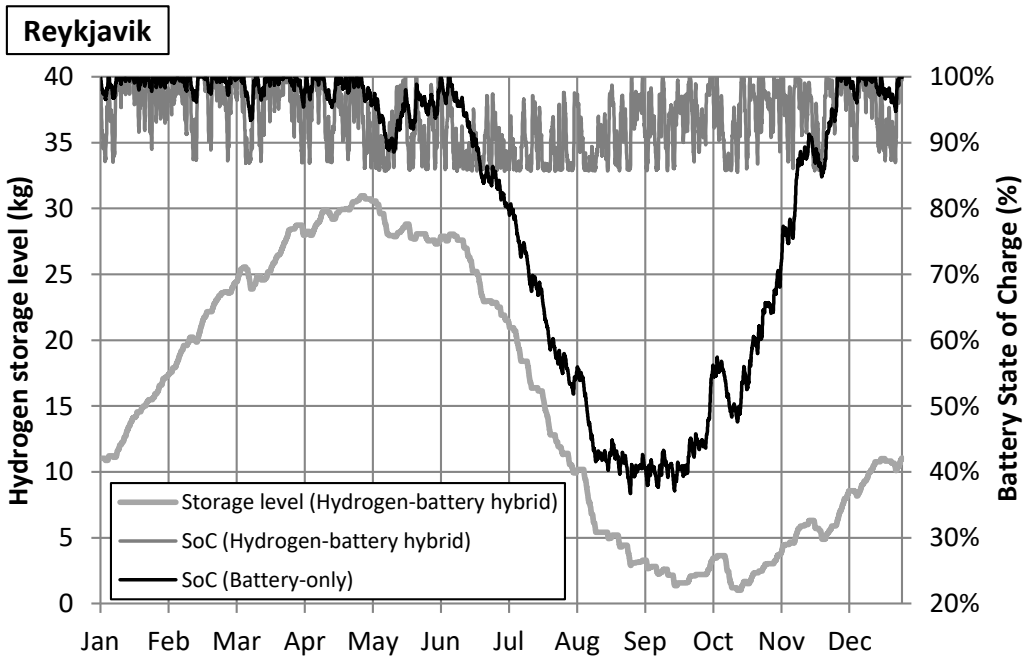
382 Figure 7: Consumption of renewable power by hybrid hydrogen-battery system

383 The wind-only site (Reykjavik) required a 4.5 kW turbine capacity and 86 batteries for its battery-only  
 384 system, and had an average battery SOC over the course of a year of 81.0% with a very low minimum SOC  
 385 of 36.7% (Table 1). It spent nearly 6 consecutive months without a full charge (Figure 8), and a total of  
 386 3,121 hrs p.a. (35.6% of the year) below 80% SOC; remaining around 40% SOC for most of August and  
 387 September. By contrast, the equivalent hybrid hydrogen-battery system required a substantial 31 kg of  
 388 hydrogen storage (reflecting the considerable seasonal storage requirements at Reykjavik), but only 20  
 389 batteries (less than a quarter of the battery-only system). The hybrid system achieved an average battery  
 390 SOC of 93.6% with a minimum SOC of 85.5% with regular full charges throughout the year, indicating the  
 391 huge benefit that the hydrogen component of the hybrid system can offer. Peak wind production occurs  
 392 in winter, so the hydrogen storage level reaches a maximum at the end of April before emptying over the  
 393 summer then reaching its minimum level in October before filling again over the winter (Figure 8), *i.e.* the  
 394 inverse behaviour of the PV powered system in Phoenix. The battery SOC was a little lower in summer  
 395 when wind availability was reduced, but remained above 85% SOC throughout. The relatively low capacity  
 396 power source (4.5 kW) compared with Phoenix reflects the high capacity factor for wind power in  
 397 Reykjavik versus solar power in Phoenix.

398

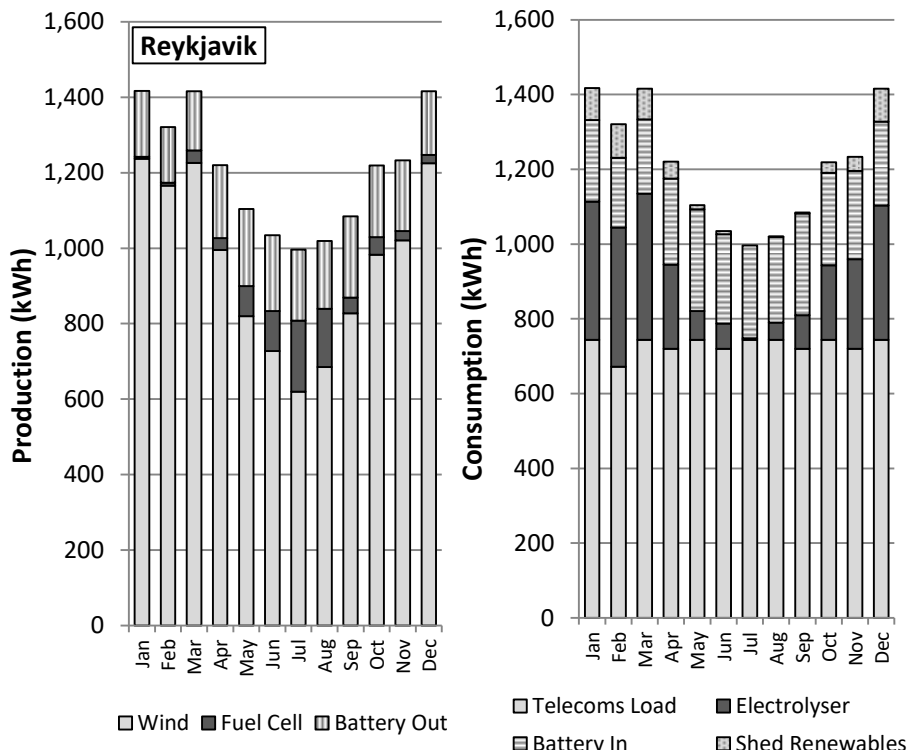
399 Electrolyser operation occurred mainly in winter to fill the store with excess wind energy (Figure 9), with  
 400 2,439 kWh overall sent to the electrolyser versus 2,588 kWh sent to the battery (*i.e.* 48.5% of the total  
 401 sent to storage, Table 2). This increased use of the electrolyser, resulting from the more pronounced  
 402 seasonal variation in wind generation than the seasonal variation in PV generation for Phoenix, combined  
 403 with a reduction in battery usage as wind generation continued overnight, demonstrates the prominent  
 404 role that the hydrogen component must play in Reykjavik, with the electrolyser actually capturing more  
 405 surplus wind than the battery during the winter months. A higher average electrolyser runtime of 6.4  
 406 hours per start-up indicates that excess wind tends to occur for longer periods than for PV systems. Fuel  
 407 cell operation occurred mainly during the summer to overcome the shortfall in wind production, with the  
 408 majority (526 kWh) used to power the telecoms load directly and the remainder (215 kWh) to recharge  
 409 the depleted battery. A lower average fuel cell runtime of 3.2 hours per start-up occurred as generation  
 410 from wind is more continuous than from PV, allowing battery SOC to be returned above its lower limit  
 411 more quickly. The continued generation from wind overnight also meant that 69% of the telecom power  
 412 requirement could be met directly by the power source (Figure 6), with 52% of wind generation being  
 413 used by the telecoms load directly (Figure 7). This reduced battery operation suggests that batteries  
 414 should last longer in wind-based hybrid systems relative to PV-based applications. The amount of  
 415 curtailed renewables was limited to 480 kWh (4.2% of total wind production) and occurred primarily in

416 the winter. This is about one quarter of the 1,928 kWh of curtailment required in the equivalent battery-  
 417 only system (16.7% of total production) where the battery remains at 100% SOC for most of the winter  
 418 months, unable to accept any excess wind.



419

420 Figure 8: Hydrogen storage level and battery SOC variations (Reykjavik)

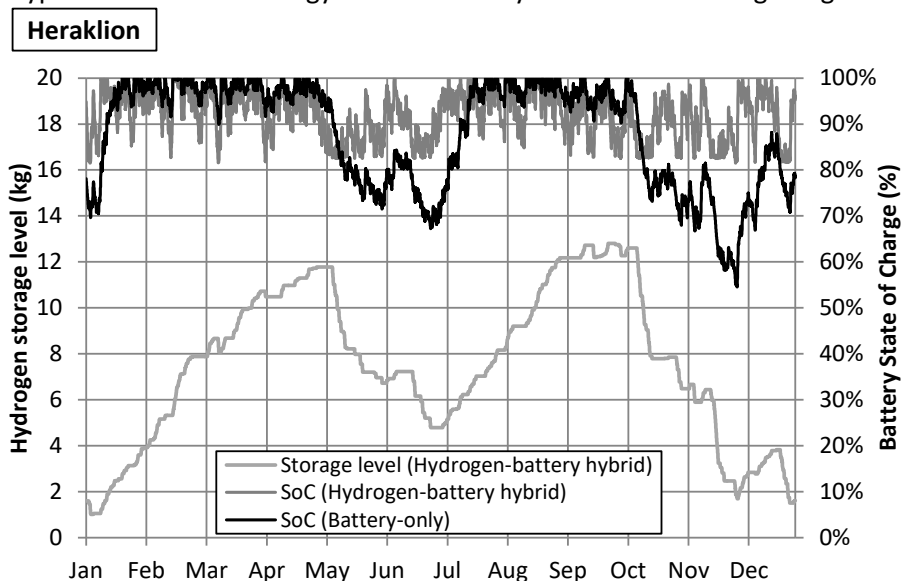


421

422 Figure 9: Monthly variations in electricity production and consumption (Reykjavik)

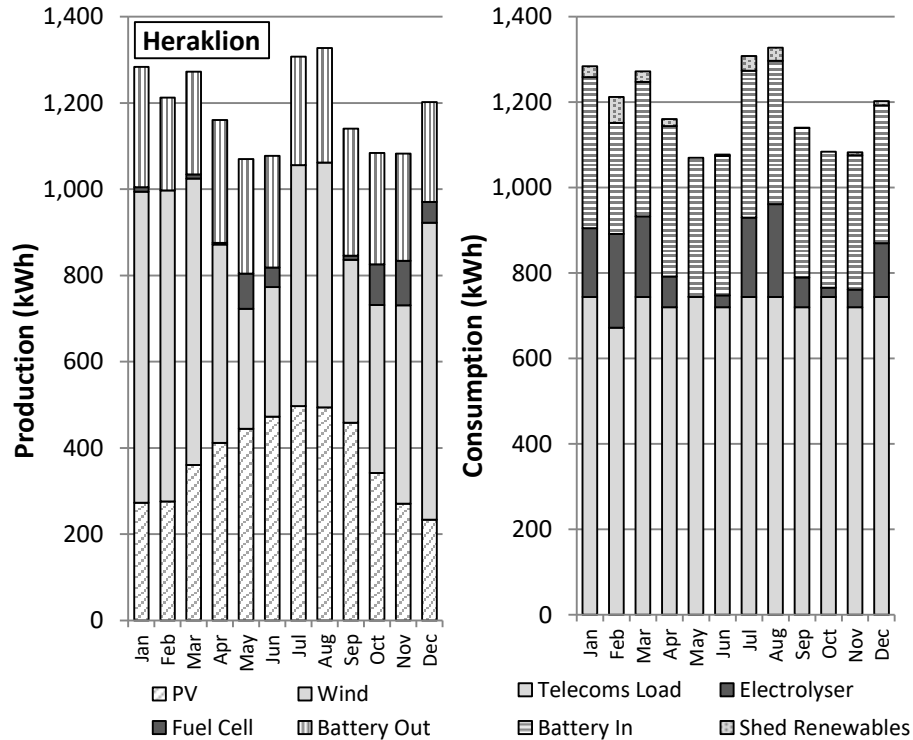
423 The site with good solar and wind resources (Heraklion) required a similar size wind turbine to Reykjavik  
 424 (4.75 kW) and a relatively small PV array (3 kW) compared with Phoenix (Table 1). This dual generation  
 425 system had the least electricity generation requirement when compared with the other two sites (Table  
 426 2). The hybrid storage system needed a broadly similar number of batteries to Reykjavik but a much  
 427 reduced hydrogen storage requirement of only 13 kg. Having two distinct power sources led to two peaks  
 428 in hydrogen store level per year (Figure 10); one occurring at the end of April due to high wind power  
 429 production over the winter, and another at the end of September due to high PV yield in the summer. The  
 430 system achieved an average battery SOC of 92.0% with a minimum SOC of 81.5% and regular full charges,  
 431 while the equivalent battery-only system required 63 batteries and achieved an average SOC of 87.9%  
 432 and a much lower minimum SOC of 54.5%. This battery-only system would spend nearly 4 months without  
 433 a full charge, and 2,820 hrs *p.a.* (32.2% of the year) below 80% SOC.

435 Electrolyser operation occurred in the summer and winter months to capture the excess PV and wind  
 436 respectively, and the average runtime of 5.1 hours per start-up is about midway between the values  
 437 obtained for Phoenix and Reykjavik. Fuel cell operation occurred mainly in the spring and autumn to fill  
 438 the valleys in the renewable generation profile (Figure 11). The low average fuel cell runtime of 3.4 hours  
 439 per start-up was nearly the same as for Reykjavik, reflecting shorter periods of low renewables generation  
 440 than for a system powered by PV alone. Battery throughput was higher than for the wind-only site  
 441 (Reykjavik) with more overnight discharging, but lower than for the PV-only site (Phoenix). 62% of the  
 442 telecom power requirement could be met directly by the renewable power sources (Figure 6), with 50%  
 443 of renewable generation being used by the telecoms load directly (Figure 7); both figures are between the  
 444 values for Phoenix and Reykjavik, but closer to the values for Reykjavik. The required curtailment level  
 445 was very low, only 213 kWh (2.0% of total generation), which amounts to about one-fifth of the 1,013  
 446 kWh that must be shed by the equivalent battery-only system for this site. Hence a hybrid system that  
 447 can access two types of renewable energy resource is very effective at utilising the generated electricity.



448

449 Figure 10: Hydrogen storage level and battery SOC variations (Heraklion)



450

451 Figure 11: Monthly variations in electricity production and consumption (Heraklion)

452 **5. Conclusions**

453 This analysis has shown that a combination of hydrogen and battery technologies in a hybrid configuration  
 454 can provide power continuously for a telecom load from an off-grid PV and/or wind power source.  
 455 Substantial storage facilities are needed to provide power during lulls in supply from the power source,  
 456 but the proposed hybrid configurations should enable more reliable and longer-lasting systems than  
 457 conventional battery-only systems. For the three distinct locations analysed, the identified capacities  
 458 required for the renewable power source, hydrogen store and battery store vary significantly but the  
 459 ranges are sufficiently narrow to invite a modular design approach for developing a hybrid system product  
 460 for global application.

461

462 The integration of on-site hydrogen generation and storage enables off-grid renewables to be harnessed  
 463 more effectively and battery SOC to be much more tightly controlled (so maximizing battery life  
 464 expectancy and useful capacity despite the inherent temporal variation in the renewable energy supply).  
 465 The oversizing of PV / wind turbine capacities often needed in battery-only systems to avoid long periods  
 466 at low SOC can be reduced, as can the wasted renewables encountered during periods of the year with  
 467 high renewables availability. Only a relatively small electrolyser (1.6kW) and fuel cell (1kW) are required;  
 468 the hydrogen store does not lose energy through self-discharge and low states of charge do not adversely  
 469 affect its life. Hence an electrolyser/store/fuel-cell system can be used to extend battery life (the critical  
 470 component in off-grid systems) by absorbing the seasonal variation in renewable supply and allowing the  
 471 batteries to cycle within their optimal SOC range year-round. This separation of conversion and storage  
 472 components means that storage capacity, unlike for batteries, can be increased without the need to resize  
 473 the electrolyser and fuel cell. The hydrogen system also helps ensure telecom reliability by providing  
 474 temporary backup power in case of failure of the PV, wind or battery components. Hydrogen storage  
 475 levels can be measured accurately remotely to provide precise estimates of remaining runtime, whereas



476 battery SOC can be difficult to measure accurately. Also the decreased requirement for batteries relative  
477 to a battery-only system reduces the use of battery chemicals, many of which are toxic.

478  
479 Within a hybrid system, the high round-trip efficiency of batteries makes them suitable for daily cycling,  
480 particularly in PV-powered systems with no overnight supply. They improve system efficiency and hence  
481 reduce the PV/wind power capacities that would otherwise be required by a hydrogen-only system. Also  
482 the battery store acts to reduce the number of electrolyser / fuel cell start-ups, absorbs transients and it  
483 is more compact than a hydrogen storage facility. Hybrid systems are more efficient than diesel  
484 generators, do not require regular deliveries of diesel (or hydrogen), respond rapidly to the varying output  
485 of renewables, and operate readily at the low loads frequently encountered with PV/wind power sources  
486 with increased rather than reduced efficiency. However, it should be noted that any variation in the  
487 assumed steady load of the application (e.g. due to seasonal weather variations) may require an  
488 adjustment of component sizes.

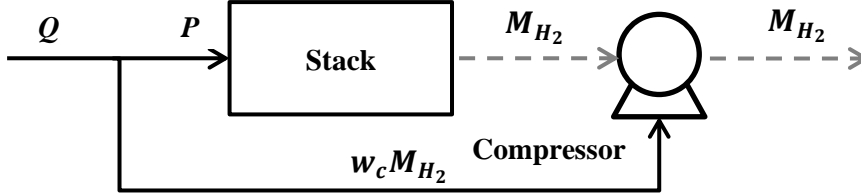
489  
490 The hybrid hydrogen-battery concept has been analysed by developing and using an hourly model to  
491 investigate the sizing and operation of a PV-powered system (Phoenix), a wind-powered system  
492 (Reykjavik) and a combined PV and wind-powered system (Heraklion). When compared with a battery-  
493 only system, the hydrogen technologies serve to maintain a high SOC year-round, irrespective of the  
494 temporal variations in renewable power generation, and to substantially reduce the number of batteries  
495 required. The role of the hydrogen component is to extend battery life by managing the SOC level by on  
496 both short term and long term timescales. This ability is very advantageous in locations with a high  
497 seasonal variation (e.g. Reykjavik) where battery-only systems otherwise need to survive six months  
498 without a full charge, but also in PV-powered systems which experience daily battery cycling due to the  
499 lack of overnight supply, and benefit from performing this cycling at high SOC. Where feasible a dual  
500 PV/wind-powered hybrid system can smooth renewable electricity generation throughout the year, which  
501 results in reduced capacity requirements for hydrogen storage and renewable power sources. Finally,  
502 when compared with delivered hydrogen solutions, the carbon footprint of the proposed hybrid approach  
503 is very attractive because it is based entirely on renewable energy - this is most important in the context  
504 of decarbonising energy use in the telecom sector.

505  
506

507  
508  
509  
510  
511

## Appendix A: Subtracting Compressor Work from Electrolyser Power

The model accounted for the compressor work as follows.



512  
513  
514  
515  
516

The energy required to operate the compressor was subtracted from the system power  $Q$  sent for electrolysis before the remainder  $P$  was sent to the electrolyser stack, *i.e.*

$$P = Q - 3,600w_cM_{H_2} \quad (\text{A. 1})$$

517  
518  
519  
520  
521  
522  
523

where  $M_{H_2}$  is the mass flowrate of hydrogen produced by the electrolyser ( $\text{kg s}^{-1}$ ), the compressor work  $w_c$  is  $4.35 \text{ kWh kg}^{-1}$  and  $P$  and  $Q$  are measured in kW. The model here considered the compressor to operate continuously; in practice a buffer tank could be used to allow intermittent compression up to the high-pressure tank.  $M_{H_2}$  can be found from the electrolyser stack efficiency  $\eta$  (electrolyser BOP drain is low enough to be ignored here), stack power  $P$  and the Higher Heating Value (HHV) of hydrogen ( $141.8 \text{ MJ/kg}$ ):

$$M_{H_2} = \frac{\eta}{1,000HHV}P \quad (\text{A. 2})$$

524  
525

Stack efficiency  $\eta$  is related to the stack voltage  $V$  by:

$$\eta = \frac{E^0}{V} \quad (\text{A. 3})$$

526  
527  
528  
529  
530

where  $E^0$  is the thermoneutral stack voltage ( $8.88 \text{ V}$  for a stack with six cells). Here the stack voltage is taken to be related to the stack current through a simple linear relationship (Figure 2); a reasonable approximation across most of the operating range, except for a slight under-prediction of current at low voltages. Hence the stack power  $P$  can be written as:

$$P = \frac{VI}{1000} \\ P = (aV + b)V \quad (\text{A. 4})$$

531  
532  
533  
534

where the values of  $a$  and  $b$  for the current-voltage relationship in Figure 2 are  $0.05 \text{ kW V}^{-2}$  and  $-0.456 \text{ kW V}^{-1}$  respectively. This gives four equations for the four unknowns  $\eta$ ,  $P$ ,  $M_{H_2}$  and  $V$ .  $M_{H_2}$  can be eliminated from (A. 1) **Error! Reference source not found.** and (A. 2) to give:

$$P = \frac{Q}{1 + \frac{3.6w_c}{HHV}\eta} \quad (\text{A. 5})$$

535  
536

Eliminating  $V$  from (A. 3) and (A. 4),

$$P = \left( a \frac{E^0}{\eta} + b \right) \frac{E^0}{\eta} \quad (\text{A. 6})$$

537

538  $P$  can be eliminated from (A. 5) and (A. 6) to give:

$$\frac{Q}{1 + \lambda\eta} = (aE^0 + b\eta) \frac{E^0}{\eta^2} \quad (\text{A. 7})$$

539

540 where, for convenience,

$$\lambda = \frac{3.6w_c}{HHV} \quad (\text{A. 8})$$

541

542 This yields a quadratic for  $\eta$ , which can be solved to give:

$$\eta = \frac{-(aE^{0^2}\lambda + bE^0) + \sqrt{(aE^{0^2}\lambda + bE^0)^2 - 4aE^{0^2}(bE^0\lambda - Q)}}{2(bE^0\lambda - Q)} \quad (\text{A. 9})$$

543

544 The stack efficiency  $\eta$  is plotted vs. stack power  $P$  as shown in Figure 2, increasing at part-load from 75%  
 545 at a stack power of 1.6 kW. To determine the effect of compressor work on system performance, the  
 546 system efficiency  $\mu$  is defined as:

$$\mu = \frac{P\eta}{Q} \quad (\text{A. 10})$$

547

548 This yields the following expression for  $\mu$ :

$$\mu = \frac{-(aE^{0^2}\lambda - bE^0) + \sqrt{(aE^{0^2}\lambda - bE^0)^2 - 4aE^{0^2}Q}}{2Q} \quad (\text{A. 11})$$

549

550 This is plotted vs. system power  $Q$  in Figure 2, and is about 70% at a system power of 1.6 kW (note the  
 551 corresponding stack power  $P$  is less than this), rising as system power falls. System efficiency continues  
 552 to increase as system power decreases because the power used for compression decreases as the  
 553 hydrogen flowrate decreases.

554

555

- [1] International Energy Agency, "Technology Roadmap: Solar Photovoltaic Energy," Paris, 2014.
- [2] International Energy Agency, "Africa Energy Outlook," Paris, 2014.
- [3] Fuel Cell Today, "Fuel Cells and Hydrogen in China," 2012.
- [4] W. Margaret Amutha and V. Rajini, "Techno-economic evaluation of various hybrid power systems for rural telecom," *Renewable and Sustainable Energy Reviews*, vol. 43, p. 553–561, 2015.
- [5] G. Bruni, S. Cordiner, V. Mulone, A. Giordani, M. Savino, G. Tomarchio, T. Malkow, G. Tsotridis, S. Bodker, J. Jensen, R. Bianchi and G. Picciotti, "Fuel cell based power systems to supply power to Telecom Stations," *International Journal of Hydrogen Energy*, vol. 39, no. 36, p. 21767–21777, 2014.
- [6] K.-A. Adamson and C. Wheelock, "Off-Grid Power for Mobile Base Stations," Navigant Consulting, Inc, 2013.
- [7] R. Wagner, "Chapter 7 – Stationary applications. I. Lead-acid batteries for telecommunications and UPS," in *Industrial Applications of Batteries*, M. Broussely and G. Pistoia, Eds., Amsterdam, Elsevier B.V., 2007, p. 395–454.
- [8] S. S. Misra, "Advances in VRLA battery technology for telecommunications," *Journal of Power Sources*, vol. 168, no. 1, p. 40–48, 2007.
- [9] E. Varkaraki, N. Lymberopoulos and A. Zachariou, "Hydrogen based emergency back-up system for telecommunication applications," *Journal of Power Sources*, vol. 118, no. 1-2, p. 14–22, 2003.
- [10] Fuel Cell Today, "First Sale of Acta's Integrated Fuel Cell–Electrolyser Backup Power System," 28 May 2013.
- [11] International Energy Agency, "Photovoltaic Power System Programme Implementing Agreement on Photovoltaic Power Systems: Task 3 - Testing of batteries used in stand-alone PV power supply systems. Report IEA PVPS T3-11," IEA PVPS, Paris, 2002.
- [12] J. Runyon, "Keeping up with energy storage," *Renewable Energy World*, vol. 17, no. 4, pp. 60-68, 2014.
- [13] J. Schiffer, D. U. Sauer, H. Bindner, T. Cronin, P. Lundsager and R. Kaiser, "Model prediction for ranking lead-acid batteries according to expected lifetime in renewable energy systems and autonomous power-supply systems," *J. Power Sources*, vol. 168, no. 1, p. 66–78, 2007.

- [14] S. Hua, Q. Zhou, D. Kong and J. Ma, "Application of valve-regulated lead-acid batteries for storage of solar electricity in stand-alone photovoltaic systems in the northwest areas of China," *Journal of Power Sources*, vol. 158, no. 2, p. 1178–1185, 2006.
- [15] R. Kaiser, "Optimized battery-management system to improve storage lifetime in renewable energy systems," *Journal of Power Sources*, vol. 168, no. 1, p. 58–65, 2007.
- [16] D. P. Jenkins, J. Fletcher and D. Kane, "Lifetime prediction and sizing of lead–acid batteries for microgeneration storage applications," *IET Renewable Power Generation*, vol. 2, no. 3, pp. 191–200, 2008.
- [17] G. Gómez, G. Martínez, J. L. Gálvez, R. Gila, R. Cuevas, J. Maellas and E. Bueno, "Optimization of the photovoltaic-hydrogen supply system of a stand-alone remote-telecom application," *International Journal of Hydrogen Energy*, vol. 34, no. 13, p. 5304–5310, 2009.
- [18] D. Bezmalinović, F. Barbir and I. Tolj, "Techno-economic analysis of PEM fuel cells role in photovoltaic-based systems for the remote base stations," *International Journal of Hydrogen Energy*, vol. 38, no. 1, p. 417–425, 2013.
- [19] S. Jiménez-Fernández, S. Salcedo-Sanz, D. Gallo-Marazuela, G. Gómez-Prada, J. Maellas and A. Portilla-Figueras, "Sizing and maintenance visits optimization of a hybrid photovoltaic-hydrogen stand-alone facility using evolutionary algorithms," *Renewable Energy*, vol. 66, p. Pages 402–413, 2014.
- [20] J. L. Bernal-Agustín and R. Dufo-López, "Simulation and optimization of stand-alone hybrid renewable energy systems," *Renewable and Sustainable Energy Reviews*, vol. 13, no. 8, p. 2111–2118, 2009.
- [21] P. Bajpai and V. Dash, "Hybrid renewable energy systems for power generation in stand-alone applications: A review," *Renewable and Sustainable Energy Reviews*, vol. 16, no. 5, p. 2926–2939, 2012.
- [22] A. Chauhan and R. P. Saini, "A review on integrated renewable energy system based power generation for stand-alone applications: configurations, storage options, sizing methodologies and control," *Renewable and Sustainable Energy Reviews*, vol. 38, p. 99–120, 2014.
- [23] M. Biemann, U. F. Vogt, M. Zimmermann and A. Züttel, "Seasonal energy storage system based on hydrogen for self sufficient living," *J. Power Sources*, vol. 196, p. 4054, 2011.
- [24] B. Shabani and J. Andrews, "Standalone solar-hydrogen systems powering Fire Contingency Networks," *International Journal of Hydrogen Energy*, vol. 40, no. 15, pp. 5509–5517, 2015.

- [25] P. García, J. P. Torreglosa, L. M. Fernández and F. Jurado, "Improving long-term operation of power sources in off-grid hybrid systems based on renewable energy, hydrogen and battery," *Journal of Power Sources*, vol. 265, p. 149–159, 2014.
- [26] F. Zhang, K. Thanapalan, A. Procter, S. Carr, J. Maddy and G. Premier, "Power management control for off-grid solar hydrogen production and utilisation system," *International Journal of Hydrogen Energy*, vol. 38, no. 11, p. 4334–4341, 2013.
- [27] S. G. Tesfahunegn, Ø. Ulleberg, P. J. S. Vie and T. M. Undeland, "Optimal shifting of PV and load fluctuations from fuel cell and electrolyzer to lead acid battery in a PV-H<sub>2</sub> standalone power system for improved performance and life time," *J Power Sources*, vol. 196, p. 10401, 2011.
- [28] Future-E, "Future-E Fuel Cell Systems: Jupiter Product Family," [Online]. Available: [http://future-e.de/data/mediapool/futuree\\_jupiter\\_family\\_dina4-4k-rgb.pdf](http://future-e.de/data/mediapool/futuree_jupiter_family_dina4-4k-rgb.pdf). [Accessed April 2015].
- [29] D. Scamman, H. Bustamante, S. Hallett and M. Newborough, "Off-grid solar-hydrogen generation by passive electrolysis," *International Journal of Hydrogen Energy*, vol. 39, no. 35, p. 19855–19868, 2014.
- [30] "Hybrid Optimization Model for Electric Renewables," [Online]. Available: <http://www.homerenergy.com>. [Accessed 18 December 2013].
- [31] NASA, "Surface meteorology and Solar Energy (SSE)," Prediction of Worldwide Energy Resource Project (POWER), [Online]. Available: <https://eosweb.larc.nasa.gov/sse/>. [Accessed 18 December 2013].
- [32] Wind & Sun Ltd, "Proven Wind Turbines," [Online]. Available: [http://windsunweb.demonweb.co.uk/Wind/wind\\_proven.htm](http://windsunweb.demonweb.co.uk/Wind/wind_proven.htm). [Accessed April 2015].
- [33] M. New, D. Lister, M. Hulme and I. Makin, "A high-resolution data set of surface climate over global land areas," *Climate Research*, vol. 21, pp. 1-25, 2000.
- [34] Rolls Battery, "4KS25P Flooded Deep Cycle Battery," [Online]. Available: <http://rollsbattery.com/public/specsheets/4KS25P.pdf>. [Accessed April 2015].